\$ STORY OF THE STO

Contents lists available at ScienceDirect

Earth and Planetary Science Letters

www.elsevier.com/locate/epsl



Pushing the boundary: A calibrated Ediacaran-Cambrian stratigraphic record from the Nama Group in northwestern Republic of South Africa



Lyle L. Nelson ^{a,*}, Jahandar Ramezani ^b, John E. Almond ^c, Simon A.F. Darroch ^d, Wendy L. Taylor ^e, Dana C. Brenner ^a, Ryan P. Furey ^a, Madison Turner ^a, Emily F. Smith ^a

- ^a Department of Earth and Planetary Sciences, Johns Hopkins University, 3400 N. Charles Street, Baltimore, MD 21218, USA
- ^b Department of Earth, Atmospheric and Planetary Sciences, Massachusetts Institute of Technology, 77 Massachusetts Avenue, Cambridge, MA 02139, USA
- ^c Natura Viva cc, PO Box 12410 Mill Street, Cape Town 8010, South Africa
- ^d Department of Earth and Environmental Sciences, Vanderbilt University, 2301 Vanderbilt Place, Nashville, TN 37235, USA
- ^e Department of Geological Sciences, University of Cape Town, Private Bag X3, Rondebosch 7701, South Africa

ARTICLE INFO

Article history: Received 2 October 2021 Received in revised form 18 January 2022 Accepted 19 January 2022 Available online 1 February 2022 Editor: B. Wing

Keywords:
Ediacaran-Cambrian boundary
Nama Group
U-Pb geochronology
carbon isotopes
Ediacaran fossils
Republic of South Africa

ABSTRACT

The Nama Group exposed on the Neint Nababeep Plateau along the Orange River in northwestern Republic of South Africa is now recognized as an expanded record of the Ediacaran-Cambrian transition that provides opportunity for an integrated stratigraphic approach in examining the geochemical and biologic evolution across this fundamental geologic boundary at unprecedented resolution. U-Pb zircon geochronology by the CA-ID-TIMS method on six intercalated volcanic ash beds in the Nama Group (from the Huns Member to the Nomtsas Formation) at this locality is used to construct a high-resolution, Bayesian, age-stratigraphic model, which allows a direct temporal calibration of the biostratigraphy and carbon isotope record from 539.63 \pm 0.15 Ma to 537.95 \pm 0.28 Ma (2 σ internal errors). Across the border in the Witputs subbasin of southern Namibia, ash beds at the base of Nudaus Formation and within the Nasep Member yielded new U-Pb ages of 545.27 \pm 0.11 Ma and 542.65 \pm 0.15 Ma, respectively. Our combined geochronology reveals the detailed depositional history of the Nama Group at a regional scale, suggesting that a relatively low sediment accumulation rate in the Kuibis Subgroup and the lower Schwarzrand Subgroup was followed by accelerated sedimentation in the upper Schwarzrand Subgroup. This is consistent with a pattern of exponential increase in subsidence typical of foreland basins. Some of the observed chemostratigraphic trends throughout the Nama Group could relate to a shift from a seawater-buffered to a sediment-buffered regime of early marine diagenesis driven by this increase in sedimentation rate.

Occurrences of soft-bodied erniettomorphs, calcified body fossils, and trace fossils within the Neint Nababeep Plateau are broadly consistent with known global biostratigraphic ranges. However, we document the youngest radioisotopically calibrated occurrences of Ediacaran-type fossils, which stratigraphically overlap with large and complex bilaterian ichnofossils, between 539.18+0.17/-0.26 Ma and 538.30+0.14/-0.14 Ma. Yet, the index fossil *Treptichnus pedum* remains undocumented from this section, and we suggest that its first regional occurrence may be younger than these strata. Despite relatively continuous and high rates of carbonate sedimentation across the Ediacaran-Cambrian boundary (as currently recognized), the upper Nama Group of the Neint Nababeep Plateau does not preserve the characteristic negative carbon isotope excursion observed within other basal Cambrian successions. One possible explanation for its absence is that this chemostratigraphic marker is not ubiquitous in all carbonate depositional environments. Alternatively, the basal Cambrian carbon isotope excursion, and perhaps the Ediacaran-Cambrian boundary as defined by the first appearance of Treptichnus pedum, might be >1 m.y. younger than currently recognized, postdating 538 Ma and, thus, suggesting a more condensed early Cambrian radiation. Difficulties in determining with confidence the first appearance datum of the index fossil Treptichnus pedum in the Nama Group highlight the challenge of a global biostratigraphic definition for the base of Cambrian and underscore the necessity of an integrated

E-mail address: lylelnelson@jhu.edu (L.L. Nelson).

^{*} Corresponding author.

stratigraphic and radioisotope geochronologic approach to understand the tempo and patterns of environmental and biologic evolution across the Ediacaran-Cambrian boundary.

© 2022 Elsevier B.V. All rights reserved.

1. Introduction

The Ediacaran-Cambrian boundary marks a critical biological transition in Earth history: the disappearance of the Ediacaran biota from the fossil record-potentially the first mass extinction of complex life—and the subsequent appearance of many metazoan clades during the Cambrian Period, including the majority of currently recognized modern phyla. The base of the Cambrian Period is defined by the first appearance of the trace fossil *Treptichnus* pedum (Brasier et al., 1994). Secondary informal markers include the first occurrences of small shelly fossils, the last occurrences of Ediacaran-type body fossils, and a large negative carbon isotope excursion, termed the BAsal Cambrian carbon isotope Excursion (BACE) (e.g., Darroch et al., 2018). As few Ediacaran-Cambrian sections have all of these markers, robust and precise correlations remain a significant problem in determining rates and global synchroneity of geochemical change and biotic turnover across this boundary. An additional potential problem is that mounting evidence demonstrates that carbon isotope excursions are not always reliable global stratigraphic markers within shallow water carbonate rocks (e.g., Higgins et al., 2018).

Currently, the Ediacaran-Cambrian boundary is temporally constrained by radioisotopic geochronology from the Nama Group near Witputs, Namibia where an ash bed below the first appearance of *Treptichnus pedum* in the Nomtsas Formation has been dated at 538.58 \pm 0.19 Ma, and strata containing fossils of erniettomorphs and *Cloudina* are constrained to <538.99 \pm 0.21 Ma (Linnemann et al., 2019). Geochronological constraints on the BACE come from the Ara Group of Oman, where an ash bed that coincides with the onset of a negative carbon isotope ($\delta^{13}{\rm C}$) excursion has been dated at 541.00 \pm 0.13 Ma (Bowring et al., 2007), and from the La Ciénega Formation of Sonora, Mexico, where a bed 20 m above the nadir of a large negative $\delta^{13}{\rm C}$ excursion has a maximum depositional age of 539.40 \pm 0.23 Ma (Hodgin et al., 2021).

Here, we present a high-resolution age-stratigraphic model based on U-Pb zircon geochronology by the chemical abrasion isotope dilution thermal ionization mass spectrometry (CA-ID-TIMS) method from eight Nama Group ash beds from southern Namibia and northwestern Republic of South Africa, which range from c. 545 to 538 Ma. Within this framework, we present calibrated high-resolution biostratigraphic and chemostratigraphic datasets from the Nama Group of the Neint Nababeep Plateau along the Orange River, allowing for examination of global biostratigraphic and chemostratigraphic correlations and trends across the Ediacaran-Cambrian transition.

2. Geological background

The Nama Group is a >1 km-thick succession of predominantly marine siliciclastic and carbonate rocks that were deposited within a late Ediacaran–early Cambrian foreland on the western margin (present-day coordinates) of the Kalahari craton. Basin formation resulted from continental flexure related to pending collision with the Rio de Plata craton to the west—the Gariep Orogen—and with the Congo craton to the north—the Damara Orogen (Fig. 1A; Germs, 1983; Germs and Gresse, 1991). Two distinct subbasins of the Nama Group have been recognized in Namibia south of Windhoek: the Zaris subbasin (north), and the Witputs subbasin (south). These are separated by the Osis arch—a paleo-high of Mesoproterozoic basement, interpreted as a peripheral bulge (Fig. 1A; Germs, 1983;

Germs and Gresse, 1991). The Kuibis Subgroup thins out over the Osis arch, suggesting that the basins were at least partially segmented by an east-northeast trending topographic high during the deposition of the basal Nama Group (Germs, 1983) with greater early subsidence in the northern subbasin. The early Cambrian Fish River Subgroup unconformably overlies the Schwarzrand Subgroup in both subbasins and was deposited as a molasse in fluvial-deltaic settings during the final stages of orogenic collision (e.g., Geyer, 2005).

Exposures of the Nama Group have also been recognized east of Windhoek in the Witvlei subbasin and in southernmost Namibia along the Orange River near the towns of Noordoewer and Aussenkehr, respectively. The exposures of the Nama Group near Noordoewer continue into the Republic of South Africa on the Neint Nababeep Plateau (Almond, 2009), and additional inliers occur to the south near the towns of Steinkopf and Springbok (Germs and Gresse, 1991; Gresse et al., 2006). Germs and Gresse (1991) interpreted all of these southernmost Nama Group exposures as part of the Vioolsdrif subbasin, separated from the Witputs subbasin by the Koedoelaagte arch, a possible east-northeast trending forebulge that was active during deposition of parts of the Schwarzrand Subgroup and the Fish River Subgroup. Alternatively, all of these exposures could be considered a southern extension of the Witputs subbasin (Germs et al., 2009). This study focuses on the Nama Group of the Neint Nababeep Plateau (Figs. 1, 2). Additional Ediacaran-Cambrian foreland basin deposits that likely correlate or partially correlate to the Nama Group occur further south in the Republic of South Africa, extending along the margin of the Kalahari craton from the Vanrhynsdorp basin along the Saldania belt to Port Elizabeth (Fig. 1A; Germs and Gresse, 1991; Gresse and Germs, 1993).

Carbon isotope chemostratigraphy of carbonate strata in the Nama Group has been one tool used for correlation regionally and globally (e.g., Saylor et al., 1998). It has been suggested that negative $\delta^{13}C$ values within carbonates of the Dabis Formation of the basal Kuibis Subgroup correlate to the end of the global Shuram carbon isotope excursion (Wood et al., 2015), which is thought to have terminated by >564.3 Ma based on Re-Os geochronology (Rooney et al., 2020). However, in South China, an ash bed U-Pb ID-TIMS date of 551.09 \pm 1.02 Ma records the recovery of a large negative excursion (Condon et al., 2005), and therefore it is possible that there are multiple distinct negative carbon isotope excursions >551 Ma (Yang et al., 2021). Regardless of whether this excursion is associated with the Shuram or with a separate, younger perturbation, the negative excursion in the Dabis Formation correlates basal carbonate strata between the Witputs and Zaris subbasins (Saylor et al., 1998; Wood et al., 2015). The overlying Zaris Formation records a recovery to positive $\acute{\delta}^{13} C$ values, peaking at $+5\%_0$ before decreasing to $\sim\!\!-1\%_0$ near the top of the unit (Saylor et al., 1998). Carbonates of the Schwarzrand Subgroup record positive δ^{13} C values ranging from \sim 0 to +3% that have been correlated to the late Ediacaran positive carbon isotope plateau (Saylor et al., 1998).

In the Zaris subbasin, the Hoogland Member of the Zaris Formation of the upper Kuibis Subgroup contains an ash bed with a U-Pb CA-ID-TIMS age of 547.36 \pm 0.23 Ma (Grotzinger et al., 1995; Bowring et al., 2007). In the Witputs subbasin, the Spitskop Member of the upper Schwarzrand Subgroup contains five ash beds dated with U-Pb CA-ID-TIMS on zircon between 540.10 \pm 0.10 Ma and 538.99 \pm 0.21 Ma, and the overlying Nomtsas Forma-

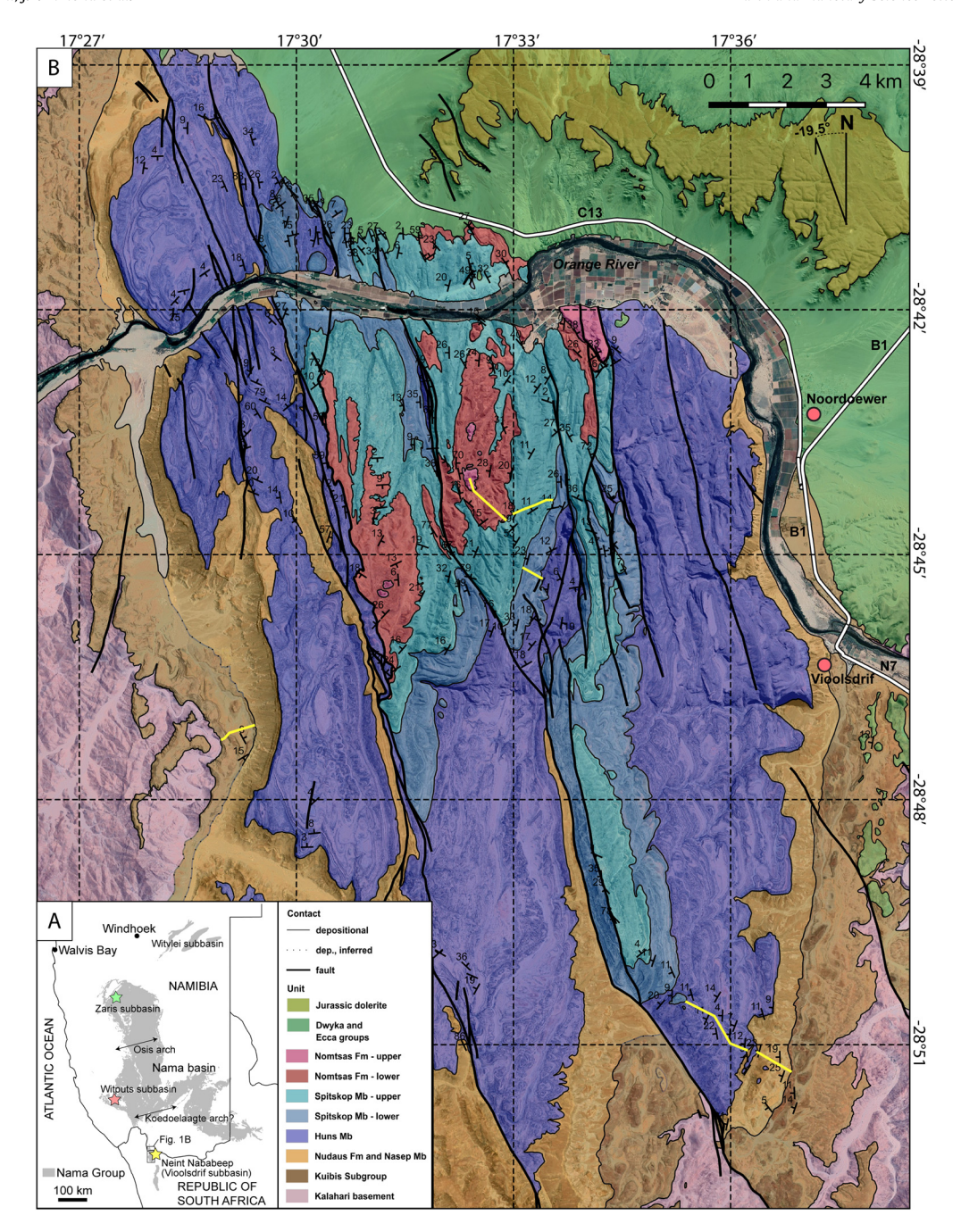


Fig. 1. A) Regional outcrop extent of late Ediacaran to early Cambrian foreland basin strata on the Kalahari Craton in southern Africa. Yellow star marks study area on the Neint Nababeep Plateau; red and green stars mark sections in Fig. 9. Compiled from geologic maps of the Geological Survey of Namibia and the Republic of South Africa Council for Geoscience. B) Geologic map of the Neint Nababeep Plateau in northwestern Republic of South Africa and southwestern Namibia. The Orange River marks the international boundary. Yellow lines are measured sections corresponding to the composite stratigraphic column in Fig. 2. (For interpretation of the colors in the figure(s), the reader is referred to the web version of this article.)

tion contains an ash bed dated at 538.58 \pm 0.19 Ma (Grotzinger et al., 1995; Linnemann et al., 2019), as well as the Cambrian index fossil *Treptichnus pedum* (Germs, 1972; Wilson et al., 2012). The Fish River Subgroup also preserves *Treptichnus pedum* (Germs, 1972; Geyer, 2005) and contains c. 540-530 Ma detrital zircon populations (Newstead, 2010; Blanco et al., 2011). A radioisotopic age gap has existed for the lower and middle Schwarzrand Subgroup.

The Nama Group preserves soft-bodied Ediacara biota of the late Ediacaran 'Nama Assemblage' (Laflamme et al., 2013) in the upper part of the Kuibis Subgroup (Kliphoek and Urikos members), including rangeomorphs and erniettomorphs (e.g., Pflug, 1970, 1972). Erniettomorphs are also found in the Nudaus, Nasep,

and Spitskop members of the Schwarzrand Subgroup, with the youngest occurrences in the upper Spitskop Member in the Witputs subbasin (above the c. 538.99 Ma date of Linnemann et al. (2019)), and in the Schwarzrand Subgroup of the Zaris subbasin (Grotzinger et al., 1995). Poorly preserved casts and molds of macroscopic tubular and annulated body fossils have been identified in both the Witputs and Zaris subbasins, and likely belong to multiple metazoan taxa, but are not readily classifiable (e.g., Germs, 1972; Darroch et al., 2016; Smith et al., 2017; Darroch et al., 2021). Carbonaceous ribbon-like compressional fossils assigned to *Vendotaenia* are preserved in the Feldshuhhorn Member of the Schwarzrand Subgroup in the Witputs subbasin (Cohen et

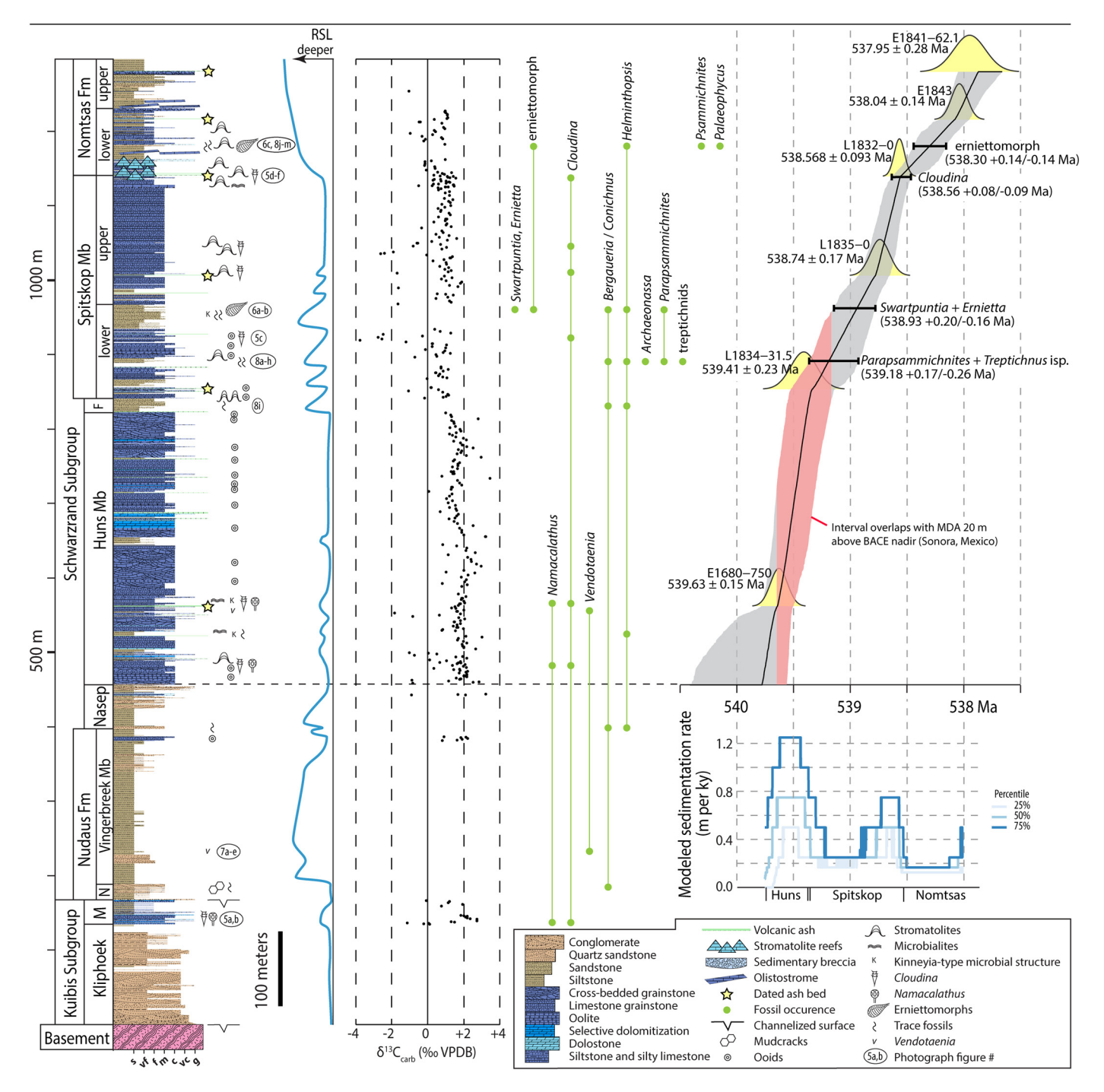


Fig. 2. Lithostratigraphy, biostratigraphy, carbon isotope chemostratigraphy, and Bayesian age-depth model of the Nama Group in the Neint Nababeep Plateau (section localities shown in Fig. 1B). Volcanic ash bed dates are weighted mean 206 Pb/ 238 U dates with internal 2σ uncertainties. The Bchron Bayesian age-depth model is presented with its median (black line) and its 95% confidence interval (grey area). Red shaded area represents overlap with maximum depositional age (MDA) for BACE from Hodgin et al. (2021). Predicted dates for fossil occurrences are calculated with their associated uncertainty using the Bchron Bayesian age-depth model. Modeled sedimentation rate does not account for delithification. M—Mooifontein; N—Niederhagen; F—Feldshuhhorn; RSL—Relative Sea Level; VPDB—Vienna-Pee Dee Belemnite.

al., 2009). Similar tubular compression fossils also occur in the lower Nudaus Formation, but have not been taxonomically assigned, as they lack branching, longitudinal creases, and organic walls that are preserved in the Feldshuhhorn population (Cohen et al., 2009).

Calcified body fossils, including *Cloudina* and *Namacalathus*, are preserved in the Omkyk Member in the Zaris subbasin (below the c. 547.36 Ma ash bed), and in the Mooifontein, Huns, and Spitskop members of the Witputs subbasin, with the last occurrence above the c. 538.99 Ma ash bed at Swartpunt (Grotzinger et al., 1995).

Cloudina also have also been reported, but not figured, from the Mara Member of the Witputs subbasin (Germs, 1972). The calcified fossil *Namapoikia*, which occurs in the Omkyk Member in the Zaris subbasin, was first interpreted as a metazoan (Wood et al., 2002), but subsequently has been reinterpreted as a microbially formed buildup (Mehra et al., 2020).

Trace fossils in the Nama Group are thoroughly reviewed by Darroch et al. (2021). Their compiled ichnostratigraphy suggests the appearance of simple, vertical plug-shaped ichnofossils in the Kuibis Subgroup and the appearance of simple horizontal trace

trails, such as Helminthopsis, Helminthoidichnites, and Archaeonassa in the lower Schwarzrand Subgroup (Nasep Member and Vingerbreek Member of the Witputs and Zaris subbasins, respectively). The more complex horizontal burrow Parapsammichnites pretziliformis was reported in the basal Spitskop Member of the Witputs subbasin (Fish River Canyon) and demonstrates complex bulldozing and active backfilling behavior (Buatois et al., 2018). Streptichnus narbonnnei was reported from the uppermost Spitskop Member of the Witputs subbasin (Farm Swartpunt) and is another complex trace fossil composed of clusters of radiating burrows extending from a central point (Jensen and Runnegar, 2005). Treptichnids occur as low as the basal Huns Member in the Witputs subbasin, and their small discontinuous burrows demonstrate relatively complex probing behavior (Jensen et al., 2000; Darroch et al., 2021). The first appearance of the more complex Treptichnus pedum (the index fossil marking the base of the Cambrian Period) occurs much higher in the strata within the Nomtsas Formation and the overlying Fish River Subgroup (Germs, 1972; Wilson et al., 2012). Scratch circles, formed by rotation of tethered organisms, have been reported from the Nudaus Formation at the Neint Nababeep Plateau and from the Spitskop Member at Farm Swartpunt (Jensen et al., 2018).

Stromatolitic and thrombolitic bioherms that form high-relief patch reefs and pinnacle reefs have been described at a number of levels within the Nama Group, including the Omkyk and Hoogland members in the Zaris subbasin and the Huns, Feldshuhhorn and Spitskop members of the Witputs subbasin (e.g., Saylor et al., 1995; Grotzinger, 2000; Grotzinger et al., 2005). These buildups are generally interpreted to have formed during flooding events and are onlapped by siltstone or silty limestone deposited during transgressive sequences. These carbonate reefs often host packstone and wackestone of Cloudina and Namacalathus fossils deposited within and between stromatolites, thrombolites, and neptunian dikes (Grotzinger et al., 2005). Bioherms are often selectively dolomitized (Saylor et al., 1995). Exhumed pinnacle reefs at Farm Swartpunt are interpreted to occur at the contact between the Huns Member and overlying Feldshuhhorn Member and reach 50 m in vertical relief (Saylor et al., 1995).

3. Methods

Fieldwork conducted throughout the Neint Nababeep Plateau in northwestern Republic of South Africa and southern Namibia included geologic mapping at variable scales using the Midland Valley FieldMove digital mapping application and the measurement of detailed stratigraphic sections with a folding meter stick (Fig. 1B). The results were integrated into a composite stratigraphic section of the Nama Group (Fig. 2). Fist-sized carbonate samples were collected at 0.5-2 m resolution for carbon and oxygen stable isotope analyses, and all identified volcanic ash beds were sampled (3 to 7 kg each) for zircon separation and U-Pb geochronology. Body and trace fossils were identified and photographed in the field, and select specimens were collected for further study and reposition at the University of Cape Town. Two additional ash beds were collected in Namibia (Witputs subbasin) from the basal Vingerbreek Member of the Nudaus Formation and from the lower Nasep Member of the Urusis Formation, respectively, on the D727 road, \sim 30 km NNE of the well documented stratigraphic section at Farm Swartpunt and \sim 180 km NNW of the Neint Nababeep Plateau. The Nasep ash bed was originally identified, but not dated, by Saylor et al. (2005). U-Pb geochronology by the CA-ID-TIMS method was carried out on single, chemically abraded zircons from the sampled ash beds. Weighted mean ²⁰⁶Pb/²³⁸U ages are reported at 95% confidence interval and in the format $\pm X/Y/Z$ Ma, where X is the internal error based on analytical uncertainties only, Y includes the tracer calibration uncertainty, and Z includes Y plus the ²³⁸U decay constant uncertainty (Jaffey et al., 1971). Carbon and oxygen isotope ratios are reported in per mil notation relative to Vienna-Pee Dee Belemnite (VPDB). Detailed analytical methods for carbon and oxygen isotope analyses, U-Pb geochronology, and Bayesian age-stratigraphic modeling are available in the Supplemental Materials.

4. Results

4.1. Stratigraphy

The Nama Group is exposed on the Neint Nababeep Plateau along the Orange River within a north-plunging syncline (Fig. 1B). Lithostratigraphic divisions of the Nama Group exposed on the Neint Nababeep Plateau broadly correspond to those of the Witputs subbasin as defined by Germs (1983), Saylor et al. (1995), and Saylor (2003) (e.g., Almond, 2009). Sedimentological and stratigraphic details of the Kuibis and lower Schwarzrand subgroups are available in the Supplemental Materials. The lowest carbonatedominated unit is the Huns Member, which is composed of \sim 220 m of cliff-forming dark blue to dark-grey weathering limestone. Much of it is cross bedded grainstone, some of which is oolitic; however, there are also thin intervals of siltstone, which are interpreted as flooding surfaces, some of which contain kinneyia-type wrinkle structures that are interpreted to be microbially mediated sedimentary forms. These flooding surfaces often preserve \sim 5 to 50 cm silicified volcanic ash beds, which form prominent orange weathering horizons. At least twenty ash beds were identified in the upper Schwarzrand Subgroup (Huns Member-Nomtsas Formation), some of which are laterally discontinuous. In the lower Huns Member, there are several horizons of microbial limestone including microbialites and low-relief stromatolites. The Huns Member is overlain by the Feldshuhhorn Member with the contact defined at the base of an interval of siltstone that marks a prominent flooding surface. Siltstone grades into fine to medium micaceous sandstone containing low angle cross stratification and channelized sandstone beds with slump folding. This is overlain by limestone of the basal Spitskop Member which contains ooids as well as a distinctive marker bed of columnar stromatolites. For mapping purposes, we informally divided the Spitskop Member into a lower and an upper submember. The lower submember of the Spitskop Member is composed of mixed limestone and siliciclastic rocks. Limestone intervals dominantly comprise grainstone, some of which is oolitic. Siliciclastic intervals are interpreted as flooding surfaces with siltstone at the base associated with maximum transgression, broadly coarsening (and shallowing) upward into micaceous sandstone. Sedimentary structures include low angle cross-stratification and slump folding within channelized sandstone beds, as well as microbially mediated kinneyia-type structures. The upper submember of the Spitskop Member is cross stratified limestone grainstone with subordinate intervals of silty limestone packstone to wackestone and a few horizons with stromatolite mounds. In sections within the eastern part of the plateau, the upper submember reaches >150 m (measured section in Fig. 2), while in the western part of the plateau it is \sim 85 m thick and dominantly comprised of stromatolitic reefs rather than grainstone.

The top of the Spitskop Member is defined by a transgressive surface and large stromatolite reefs that form high relief pinnacles and mounds (up to 10s of meters in height). These reefs are onlapped by silty limestone and siltstone, which have preferentially weathered away such that at some localities the outcrops resemble primary seafloor topographic relief (Fig. 3A, B). Reefs are formed of amalgamations of stromatolites that have morphologies ranging from large domes to conical structure, and commonly have thrombolitic cores. Siltstone, sandstone, and silty limestone of the Nomtsas Formation overlie the reefs and host carbonate clast

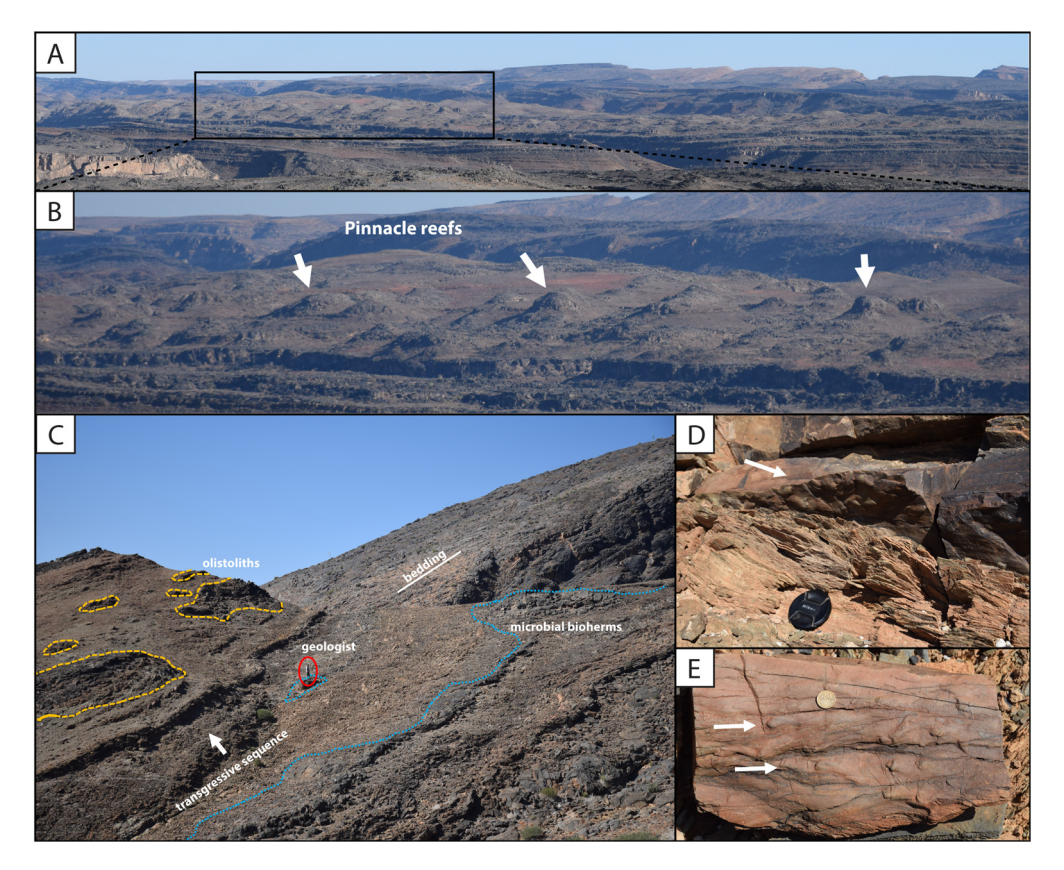


Fig. 3. Field photographs of the Nomtsas Formation. A, B) Pinnacle reefs of stromatolitic and thrombolitic bioherms weathering out of onlapping siltstone and silty limestone at the base of the Nomtsas Formation. Field of view in 3B is \sim 1 km. C) Contact between Spitskop Member and Nomtsas Formation. Bioherm build ups denoted with dashed blue line and olistoliths of limestone denoted with orange dashed line D, E) Flute marks on the base of turbidite beds within the Nomtsas Formation. Lens cap is 5.2 cm in diameter. Coin is 1.9 cm in diameter.

debrites and carbonate olistoliths (up to 20 m in diameter) that are interpreted as submarine mass transport deposits (Fig. 3C). The base of some channelized sandstone beds within this unit contain flute marks (Fig. 3D, E), and no sedimentary structures indicative of traction currents were observed. Overall, the Nomtsas Formation is interpreted to have been deposited during a transgression related to flexure of continental crust underlying the Nama foreland basin that drowned out the carbonate platform by increasing the flux of siliciclastic material. High-relief pinnacle reefs formed in the basal Nomtsas Formation as microbial stromatolites initially kept pace with increasing subsidence, but were eventually drowned out by the siliciclastic sediment and/or increasing water depth. Steep slope gradients generated from the flexure of the continental margin led to the deposition of submarine mass flow deposits, including olistostromes and sedimentary breccias. The Nomtsas Formation is the stratigraphically highest exposed unit of the Nama Group on the Neint Nababeep Plateau.

4.2. Geochronology

Our new U-Pb geochronology based on eight interstratified ash bed ages, integrated into a Bayesian age model, presents the first high-resolution chronostratigraphic framework for the entire Nama Group across southern Namibia and northwestern Republic of South Africa. Six of these ash beds are from the Schwarzrand Subgroup at the Neint Nababeep Plateau, spanning the lower Huns Member to the Nomtsas Formation, which encompasses the Ediacaran-Cambrian transition. Another two are from the lower Schwarzrand Subgroup, basal contact of the Nudaus Formation and lower Nasep Member of the Urusis Formation, in the Witputs subbasin (Figs. 2, 4, 9; Table SM2). Table 1 summarizes the age results, which range from $545.27 \pm 0.11/0.18/0.61$ Ma (Nudaus Formation)

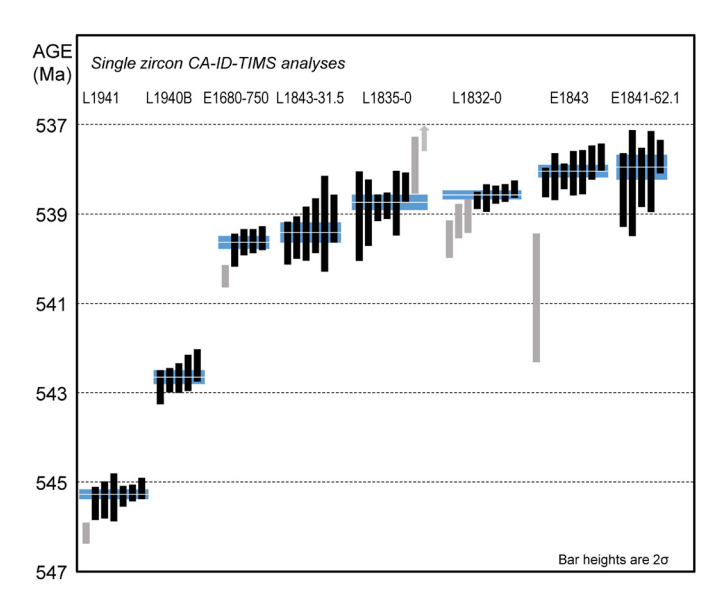


Fig. 4. Ranked age plot of the analyzed zircons from the interstratified ash beds of the Nama Group. Vertical bars are individual zircon analyses with their 2σ analytical uncertainty; black bars are analyses used in age calculation. Arrow represents the analysis plotting outside the diagram. Blue band signifies the 95% confidence level (2σ) internal uncertainty of the weighted mean age.

to 537.95 \pm 0.28/0.36/0.68 Ma (Nomtsas Member). The average analytical uncertainty of individual zircons analyses was \pm 400 kyr (0.7‰), which enabled calculation of weighted mean ages with internal uncertainties as low as \pm 100 kyr (0.2‰) in order to resolve age differences among closely spaced ash beds (Fig. 4).

Table 1Summary of calculated U-Pb dates and their uncertainties.

Sample	Latitude (N)	Longitude (E)	Unit	²⁰⁶ Pb/ ²³⁸ U Age (Ma)	Error $(2\sigma)^a$			MSWD ^b	n ^c	No.
					X	Y	Z			
Neint Nababeep Plateau, Re	public of South Afr	ica								
E1841-62.1	-28.72461°	17.53997°	Nomtsas Formation	537.95	0.28	0.36	0.68	0.98	5	5
E1843	-28.72706°	17.54244°	Nomtsas Formation	538.04	0.14	0.27	0.63	1.4	7	8
L1832-0	-28.74472°	17.54450°	Nomtsas Formation	538.568	0.093	0.17	0.60	0.95	5	8
L1835-0	-28.75117°	17.55109°	Spitskop Member	538.74	0.17	0.25	0.63	1.1	6	8
L1834-31.5	-28.75965°	17.55480°	Spitskop Member	539.41	0.23	0.33	0.66	0.60	6	6
E1680-750	-28.79168°	17.50051°	Huns Member	539.63	0.15	0.27	0.64	0.47	4	5
Witputs subbasin, Namibia										
L1940B	-27.33969°	16.69826°	Nasep Member	542.65	0.15	0.21	0.62	1.0	5	5
L1941	-27.22152°	16.79246°	Nudaus Formation	545.27	0.11	0.18	0.61	0.63	6	7

^a X-internal (analytical) uncertainty in the absence of all external or systematic errors; Y-incorporates the U-Pb tracer calibration error; Z-includes X and Y, as well as the uranium decay constant errors (Jaffey et al., 1971).

Our Bayesian age-depth model suggests that ~820 m of strata of the upper Schwarzrand Subgroup (Huns Member-Nomtsas Formation) were deposited in 1.90+0.84/-0.39 m.y. with an average sediment accumulation rate of 43.2+11.3/-13.2 cm/kyr (Fig. 2). This age-depth model does not incorporate delithification; taking into account expected sediment compaction by using carbonate parameters from Kim et al. (2018) and a 1.5-3 km range for burial depth would increase this rate by 42-66%. Our age model reveals that siliciclastic-dominated intervals (Feldshuhhorn and lower Spitskop members and Nomtsas Formation) had resolvably lower average sediment accumulation rates than carbonate-dominated intervals (Huns and upper Spitskop members) (Fig. 2). Some of this disparity may be attributed to ~40-70% more post-depositional sediment compaction in shale compared to carbonate (with parameters from Kim et al. (2018) and 1.5-3 km burial depths), but this does not account for the entire difference in modeled stratigraphic accumulation rates. Our age model incorporates a previously reported CA-ID-TIMS U-Pb date of 547.36 \pm 0.23 Ma from an ash bed in the Hoogland Member of the Zaris subbasin in Namibia (Bowring et al., 2007), which is correlative to the middle of the Mooifontein Member to the south (e.g., Germs, 1983; Grotzinger et al., 1995; Saylor et al., 1998). Along with two new ash bed dates from the Witputs subbasin in Namibia, this establishes a temporal framework for the entire Nama Group. Based on the composite age-stratigraphic model, average sediment accumulation rates for the lower Schwarzrand subgroup (Nudaus Formation and Nasep Member) are significantly lower than the upper Schwarzrand subgroup (4.3+1.0/-0.3 cm/kyr vs. 43.2+11.3/-13.2 cm/kyr), and, again, only a fraction of this difference can be attributed to lithologically variable compaction.

A noteworthy outcome of the new Nama Group chronostratigraphy is the absence of hiatuses in the upper Schwarzrand subgroup, even at the high resolution of our age model. This is particularly significant for the Spitskop Member–Nomtsas Formation boundary, which has been traditionally described as unconformable valley incisions in the Witputs subbasin (e.g., Grotzinger et al., 1995; Saylor et al., 1995). Our Bayesian age-depth model based on tightly bracketing U-Pb ages does not indicate any detectable changes in the sediment accumulation rate across the latter boundary, when compared to that of other lithologically similar stratigraphic intervals of the upper Nama Group (see Figs. 2, 4). This finding has important implications for the interpretation and placement of the Ediacaran-Cambrian boundary (see Discussion below).

4.3. Carbon and oxygen isotope chemostratigraphy

Carbon isotope (δ^{13} C) values of carbonates of the Mooifontein Member are scattered between $\sim -1\%_0$ and $\sim +3\%_0$. Within the

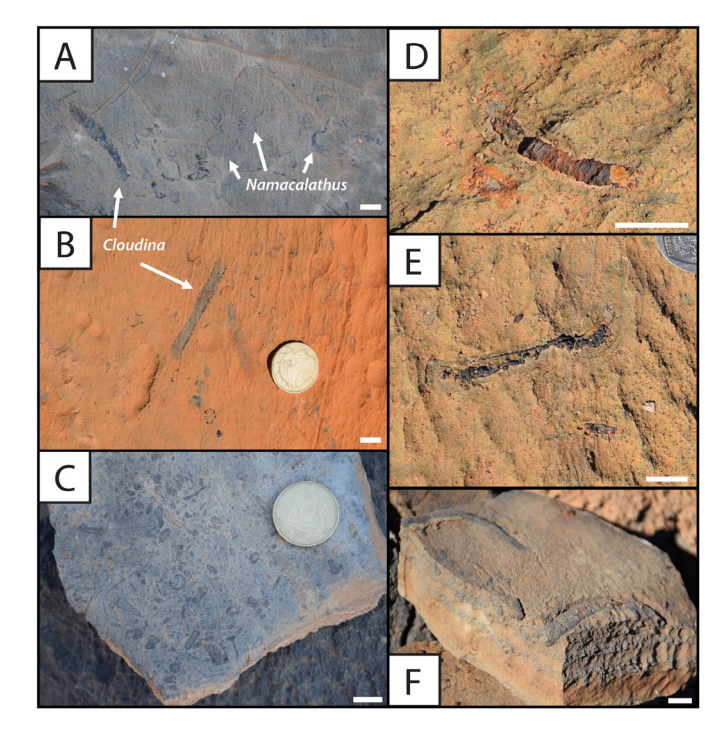


Fig. 5. Calcified body fossils from the Neint Nababeep Plateau. White scale bars are 1 cm. A, B) *Cloudina* and *Namacalathus* in the Mooifontein Member. C) Shell hash in limestone wackestone in the lower Spitskop Member with circular cross sections of broken cloudinid fossils. D–F) Cloudinid fossils in the basal Nomtsas Formation that are selectively replaced by iron oxides (likely oxidized pyrite). Specimens in (D) and (F) show characteristic cone-in-cone structure of cloudinomorphs.

Huns Member the δ^{13} C values are $\sim +2\%$, decreasing to $\sim +1\%$ near the top and staying at $\sim +1\%$ throughout the Spitskop Member and lower Nomtsas Formation (Fig. 2). Throughout much of the section, there is significant scatter, and the more negative values (>-4%) are associated with more siliciclastic-rich intervals (silty to sandy limestone or proximity to siltstone and sandstone), but these individual data points do not form consistent trends and are lithology dependent (Fig. 3), and therefore may be the result of very localized and stratigraphically confined organic carbon remineralization rather than reflecting any basin-wide negative δ^{13} C excursion. The few samples with negative δ^{13} C values have relatively enriched or depleted δ^{18} O values, which is also consistent with localized diagenetic influence, while the majority of samples show no consistent trends among δ^{13} C and δ^{18} O values (Fig. SM1).

^b MSWD-mean square of weighted deviates.

c n-number of analyses included in the calculated weighted mean date out of the total number of analyses (No.).

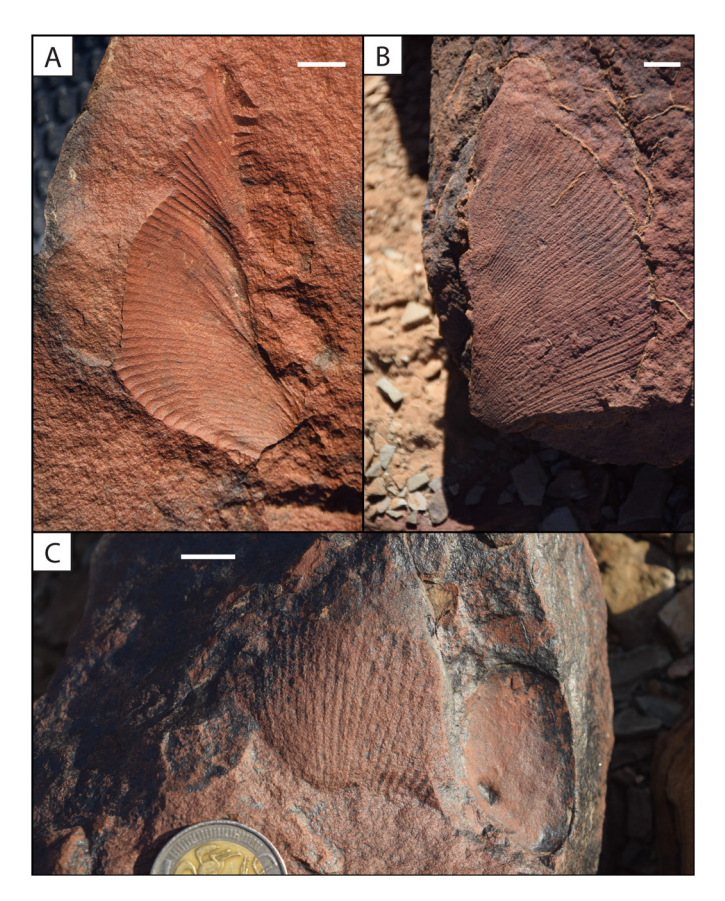


Fig. 6. Erniettomorph body fossils from the Neint Nababeep Plateau. A) Probable *Ernietta plateauensis* in the lower Spitskop Member. B) *Swartpuntia germsi* in the lower Spitskop Member. C) Indeterminate erniettomorph in the Nomtsas Formation. Scale bars are 1 cm.

4.4. Biostratigraphy

In the Nama Group outcrops of the Neint Nababeep Plateau, calcified fossils of *Cloudina* and *Namacalathus* occur in the lower limestone of the Mooifontein Member and the lower Huns Member (Fig. 5A, B; Gresse et al., 2006; Almond, 2009). Calcified tubular fossils also occur in the Spitskop Member and in the basal Nomtsas Formation, which are likely cloudinids as well, but are mostly preserved as recrystallized tubes without readily identifiable conein-cone structure (Fig. 5C–F). However, some of the tubular fossils in this interval are replaced by iron oxide and preserve characteristic cone-in-cone structure (Fig. 5D, F), and therefore are identified as *Cloudina*.

Body fossils of erniettomorphs, including Swartpuntia germsi and probable Ernietta plateauensis, are preserved in sandstone beds within the lower Spitskop Member (Fig. 6A, B) and are the first soft-bodied Ediacaran fossils to be reported in the Republic of South Africa. Erniettomorphs occur in approximately correlative strata of the Spitskop Member at Farm Swartpunt (Witputs subbasin) in Namibia (e.g., Grotzinger et al., 1995; Narbonne et al., 1997). An additional partial erniettomorph body fossil resembling Ernietta was found in the lower Nomtsas Formation, above the 538.568 \pm 0.093 Ma and below the 538.04 \pm 0.14 Ma ash beds, but is not definitively identifiable (Fig. 6C). Ribbon-like, filamentous compressional body fossils are preserved on bedding planes within siltstone to fine sandstone of the lower Nudaus Formation, as well as within the lower Huns Member (Fig. 7: Almond. 2009). These are morphologically similar to tubular fossils within the lower Nudaus Formation of the Witputs subbasin in Namibia

described by Cohen et al. (2009), and we tentatively assign them to *Vendotaenia*, although this identification will require reassessment as the taxonomic framework for Ediacaran tubular fossils improves. These filamentous fossils are associated with scratch circles (Jensen et al., 2018), and so they may have been tethered organisms. Poorly preserved casts and molds of annulated or ribbed tubular body fossils that are <1 cm in diameter occur in siliciclastic intervals of the lower Spitskop Member, but do not preserve the morphological detail for confident identification.

Ichnofossils were identified within several stratigraphic horizons, and identification follows classifications of Darroch et al. (2021). Vertical plug-shaped fossils that are assigned to either Bergaueria or Conichnus occur in the Niederhagen Member of the Nudaus Formation, the basal Nasep Member, the Feldshuhhorn Member, and siliciclastic intervals of the lower Spitskop Member. Simple bed planar trace fossils, assigned to Helminthopsis (on the basis that there is little evidence of overcrossing), occur in the Nasep, lower Huns, Feldshuhhorn, and lower Spitskop members of the Urusis Formation, and in the Nomtsas Formation (see also Gresse et al., 2006; Almond, 2009). In the lower Nomtsas Formation, densely spaced and overlapping bed-planar burrows are particularly large with widths >1 cm and lengths >10 cm (Fig. 8L, M); the lack of branching and structureless infill in these trace fossils allow tentative identification as Palaeophycus. More complex horizontal burrows that demonstrate bulldozing and active backfilling behavior are identified as Parapsammichnites pretziliformis (Buatois et al., 2018) and occur in the lower Spitskop Member in high abundance within a <5 m interval at the top of the second major siliciclastic interval (Fig. 8A-F). Dense, cross-cutting meshworks of horizontal to oblique burrows in these same slabs possessing irregularly-spaced constrictions may be attributable to Torrowangea (Fig. 8A). Archaeonassa, a sinuous horizontal trail with a wide central furrow and lateral ridges, occurs within this same interval (Fig. 8H). Larger, bilobed and unbranched trace fossils with pronounced medial grooves also occur within the Nomtsas Formation (Fig. 8J-K); however, the higher relief and the possible presence of poorly-preserved arcuate backfill (see Fig. 8K) instead suggest that these may represent Psammichnites. Recent work (e.g., MacNaughton et al., 2021) suggests that Psammichnites may be a useful biostratigraphic marker for the early Cambrian, however, we note that in the Neint-Nabeeb Plateau this ichnotaxon apparently predates the first appearance of Treptichnus pedum (see Section 5.1). One trace fossil specimen recovered from the lower Spitskop Member exhibits strings of almond-shaped probes (strongly resembling those described by Darroch et al. (2021) from the base of the Spitskop Member in Namibia; their Fig. 13F-G), which likely represent discontinuous horizontal to vertical branching off of a single concealed master burrow (Fig. 8G). Given that these burrows lack the diagnostic features of Treptichnus while representing a broadly similar (albeit less complex) behavior, these are best identified as treptichnids (see e.g., Jensen et al., 2000). Finally, one enigmatic fossil found in the Feldshuhhorn Member possesses a helical, corkscrew-type structure (Fig. 8I) and thus resembles an isolated probe belonging to the latest Ediacaran trace fossil Streptichnus narboneii (Jensen and Runnegar, 2005). However, given that the fossil exhibits sinistral twisting (rather than dextral, which is more typical of Streptichnus), the lack of any other associated burrows radiating from a single entryway, and the observation that both the tightness and angle of coiling appear to change along the length of the structure, we instead tentatively assign this fossil to Harlaniella, which is a problematic body fossil best known from late Ediacaran sections in Russia and Ukraine (Ivantsov, 2013).

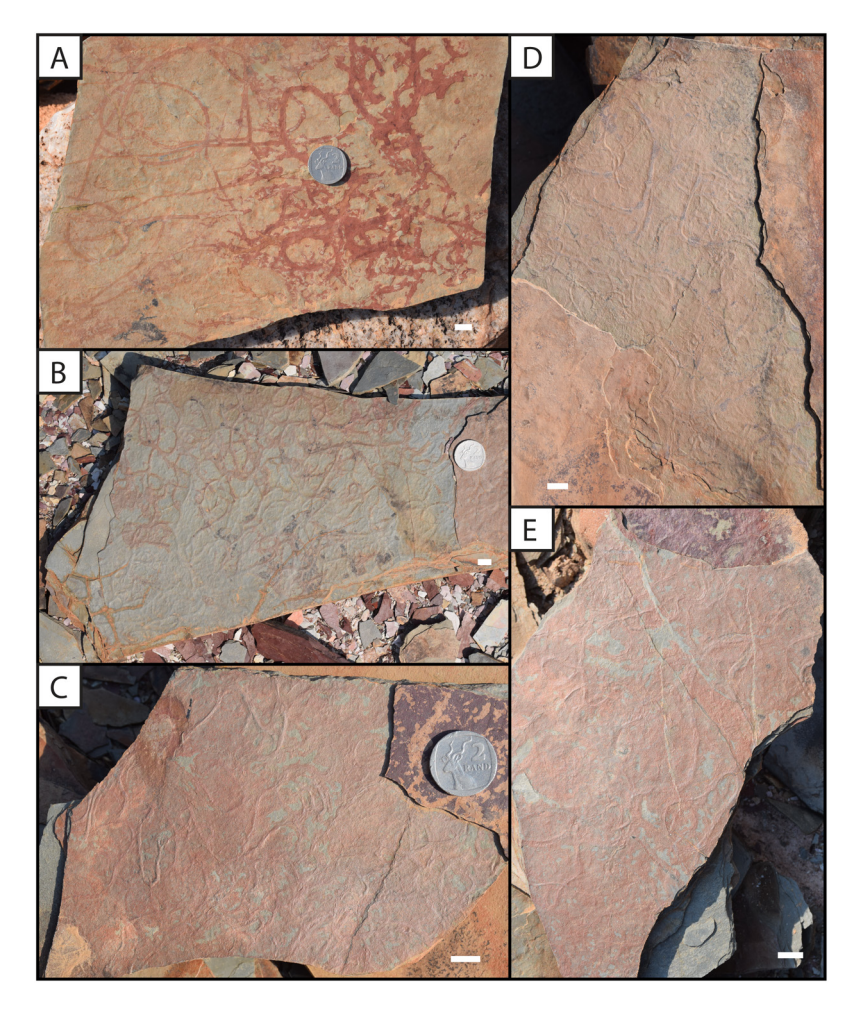


Fig. 7. Compression fossils of Vendotaenia in the Nudaus Formation from the Neint Nababeep Plateau. Scale bars are 1 cm.

5. Discussion

5.1. Placement of the Ediacaran-Cambrian boundary in the Nama Group

For decades, the Nama Group of Namibia has been recognized as a critical record of the Ediacaran-Cambrian boundary, and the ash bed ages from the Spitskop Member and Nomtsas Formation at Farm Swartpunt (Grotzinger et al., 1995; Linnemann et al., 2019) have been used for the calibration of the Geologic Time Scale (Peng et al., 2020). The consensus view has been that the base of the incised valleys of the basal Nomtsas Formation is the stratigraphic position of the Ediacaran-Cambrian boundary in Namibia (e.g., Germs, 1972, 1983; Grotzinger et al., 1995; Saylor et al., 1995). This notion is influenced by incomplete and discontinuous exposures of the lithostratigraphic boundary, as well as documentation of Treptichnus pedum (or Phycodes pedum based on previous nomenclature) in units identified as the Nomtsas Formation at Farm Swartkloofberg by Germs (1972) and at Farm Sonntagsbrunn (Grotzinger et al., 1995; Wilson et al., 2012). However, the specimens identified as "closely related to or identical with Phycodes pedum" at Swartkloofberg by Germs (1972) (their Plate 2, Fig. 5) lack clear systematic branching patterns of straight to slightly curved segments diagnostic of Treptichnus pedum (Seilacher, 2007). There has been no subsequent documentation of this fossil from the Nomtsas Formation at Swartkloofberg (e.g., Saylor and Grotzinger, 1996). Treptichnus pedum has, however, been extensively documented from the Nomtsas Formation at Farm Sonntagsbrunn by Wilson et al. (2012). These specimens are in a unit they identify as 'Valley Fill 2', which they interpret as lower shoreface facies that occur within an incised valley and below a capping sheet deposit of upper shoreface sandstone. Above the Nomtsas Formation, within the Fish River Subgroup, *Treptichnus pedum* has been well documented within the Rosenhof Member of the Gross Aub Formation (e.g., Germs, 1972; Crimes and Germs, 1982; Geyer and Uchman, 1995; Geyer, 2005). Beyond the ichnofossil record, the placement of the Ediacaran-Cambrian boundary at the base of the Nomtsas valley incision has been justified based on the last occurrences of Ediacaran-type fossils in the underlying Spitskop Member, and by the absence of the BACE in the upper Nama Group, which has been attributed to the hiatus at the unconformity (e.g., Grotzinger et al., 1995).

This study demonstrates that the Nomtsas Formation on the Neint Nababeep Plateau is associated with marine transgression rather than valley incision, and at this locality there is no demonstrable unconformity at the contact between the Spitskop Member and the Nomtsas Formation. Instead, there is continuous deposition, transitioning from carbonate shelf environment to a deeper marine environment dominated by siliciclastic sedimentation. This is supported by a number of lines of evidence including: 1) development of large pinnacle microbial reefs at this contact; 2) the absence of any paleo-relief or evidence of incision; 3) the presence of mass transport deposits and turbidites along with the absence of sedimentary structures indicative of traction currents in the Nomtsas Formation; and 4) the high-resolution U-Pb geochronology that demonstrates no resolvable hiatus. While valley incision clearly occurs at the base of the Nomtsas Formation at both Farm Swartkloofberg and in the 'Valley Fill 1' unit at Farm Sonntagsbrunn, in both cases, valley fill sediments were deposited below wave base

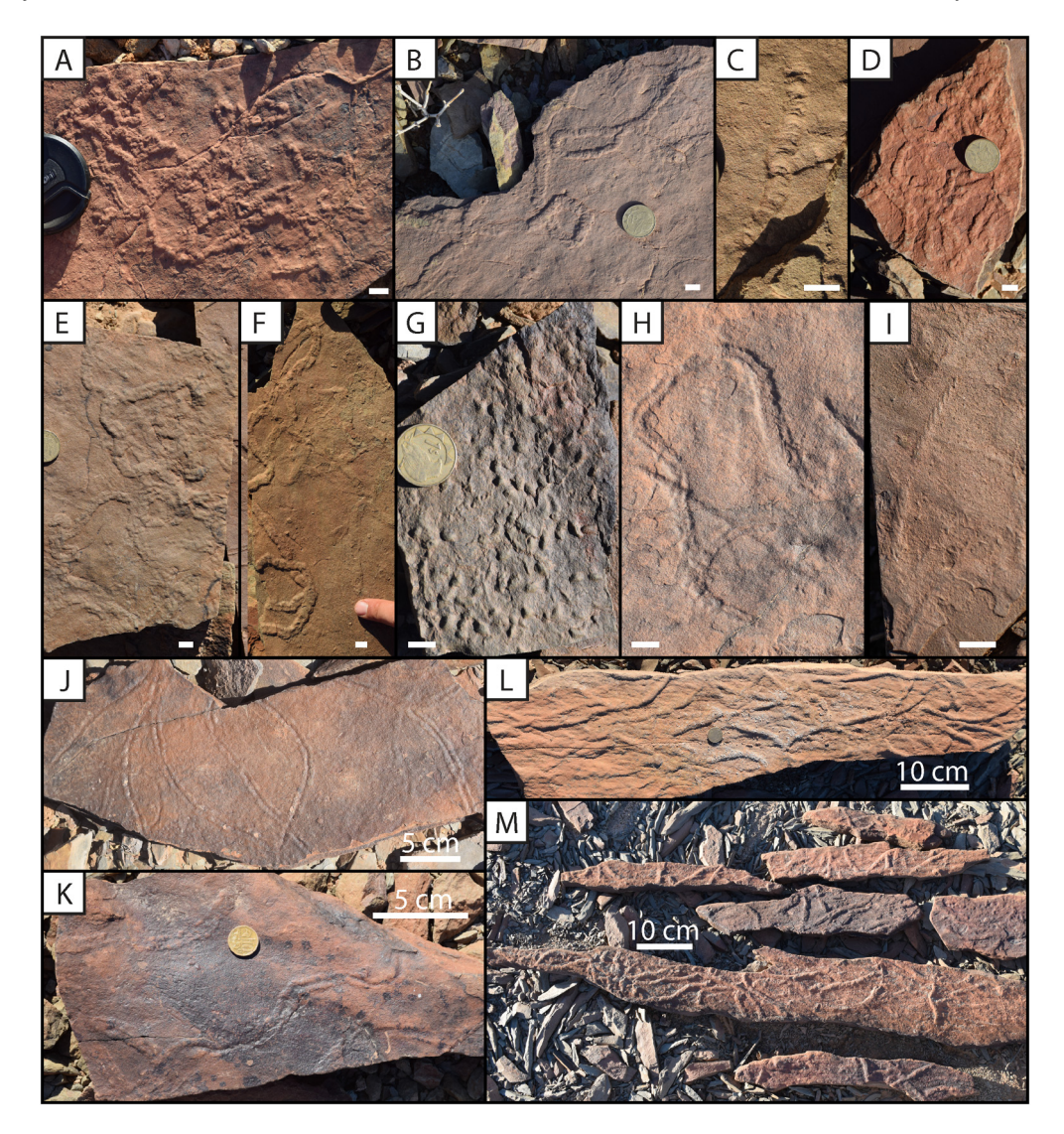


Fig. 8. Trace fossils in the lower Spitskop Member and lower Nomtsas Formation from the Neint Nababeep Plateau. Scale bars are 1 cm unless otherwise noted. A–F) Parapsammichnites pretziliformis in the lower Spitskop Member exhibiting characteristic overcrossing behavior, and arcuate active backfill. Irregular meshwork of horizontal burrows in the center of A exhibiting irregular constrictions is potentially attributable to Torrowangea. G) Probable treptichnids in the lower Spitskop Member, preserved as strings and arcs of individual almond-shaped 'probes'. H) Archaeonassa in the lower Spitskop Member. I) Unidentified helical structure in the Feldshuhhorn Member potentially attributable to the body fossil Harlaniella. J–K) Probable Psammichnites in the Nomtsas Formation. L–M) Large, planar, unbranched and crosscutting trace fossils in the Nomtsas Formation with structureless infill, identified as Palaeophycus.

and are dominated by suspension sedimentation of mud and silt accompanied by gravity-driven flows of sand and carbonate-clast conglomerate and diamictite (Saylor and Grotzinger, 1996; Wilson et al., 2012). Thus, it is reasonable that these were localized submarine channels formed by mass wasting during margin flexure and marine transgression (Saylor and Grotzinger, 1996; Wilson et al., 2012), rather than by a fluvial system related to a regional unconformity. This is consistent with our interpretations of the Neint Nababeep Plateau, as well as recent geochronology at Swartpunt and Swartkloofberg (Linnemann et al., 2019).

Since no definitive specimens of *Treptichnus pedum* have been found in the Nomtsas Formation at Swartkloofberg or the Neint Nababeep Plateau, it may be argued that the biostratigraphically defined Ediacaran-Cambrian boundary occurs still higher in the section, younger than 537.87+0.18/-0.21 Ma. While there are clear occurrences of *Treptichnus pedum* within the 'Valley Fill 2' unit at Farm Sonntagsbrunn, given the stratigraphic interpretation of the Nomtsas as part of a transgressive systems tract, it is possible that the shoreface 'Valley Fill 2' and 'Upper Nomtsas Member' units of Wilson et al. (2012) are not directly correla-

tive to the dated Nomtsas Formation at Farm Swartkloofberg or the Neint Nababeep Plateau, and instead are younger than 537.9 Ma, and genetically related to the orogenic molasse of the Fish River Subgroup. This interpretation is further supported by the presence of a probable erniettomorph in the sandstones of the Nomtsas Formation and Cloudina in the limestones of the basal Nomtsas Formation at the Neint Nababeep Plateau, which indicate these Ediacaran-type fossils continue into the Nomtsas Formation. On the other hand, it has been documented that cloudinids may overlap in their stratigraphic range with the earliest Cambrian fossil assemblages (e.g., small shelly fossil zone I) without a sharp biotic turnover (Yang et al., 2016; Zhu et al., 2017). Globally, outside of the Nama Group, the first appearance datum of Treptichnus pedum is not well constrained by radioisotopic age constraints, and a biostratigraphically defined boundary younger than 537.9 Ma is compatible with current data. Alternatively, since the first appearance of Treptichnus pedum was originally chosen to mark the base of the Cambrian Period in an attempt to place the boundary close to the earliest occurrence of the first unquestionable bilaterian fossil, perhaps the boundary should be placed much lower in the

Nama Group where other complex, bilaterian ichnofossils occur, as suggested by Geyer (2005). If the occurrence of *Parapsammichnites pretziliformis* in the lower Spitskop Member, or the stratigraphically lower occurrence of *Treptichnus* isp. in the lower Huns of the Witputs subbasin (Jensen et al., 2000), is taken as such earliest occurrence, then the interval between 539.18+0.17/-0.26 Ma and 538.30+0.14/-0.14 Ma—the last occurrence of an erniettomorph—may be hypothesized as an Ediacaran-Cambrian 'transition interval'. Overall, the age-calibrated fossil assemblages of the upper Nama Group at the Neint Nababeep Plateau further underscore the difficulties in arriving at a unified, global, biostratigraphic definition of the Ediacaran-Cambrian boundary.

5.2. Chemostratigraphy of the Nama Group

At a number of localities globally, a large negative carbon isotope excursion, the BACE, has been shown to immediately predate the first appearance of *Treptichnus pedum* and/or postdate the last occurrence of Ediacaran-type fossils (e.g., Narbonne et al., 1994; Brasier et al., 1996; Zhang et al., 1997; Corsetti and Hagadorn, 2000; Smith et al., 2016). Therefore, the BACE is thought to mark the Ediacaran-Cambrian boundary and has been linked to environmental perturbation and, possibly, extinction (e.g., Amthor et al., 2003; Smith et al., 2016; Darroch et al., 2018; Hodgin et al., 2021), even though its absolute age has not been independently well constrained. While a negative carbon isotope excursion occurs in carbonates of the basal Kuibis Subgroup (e.g., Saylor et al., 1998; Wood et al., 2015), there is no negative carbon isotope excursion preserved within \sim 780 m of carbonate deposits of the upper Schwarzrand Subgroup that spans 1.74 m.y. from c. 539.8 to 538.0 Ma, despite a high average sedimentation rate of \sim 44 cm/kyr (apparently higher in carbonate-dominated intervals) and no clear hiatuses (Fig. 2).

Two possible explanations for the absence of the BACE in the upper Nama Group are: 1) this excursion is younger than carbonates of the Schwarzrand Subgroup, or, 2) Schwarzrand Subgroup carbonates record the composition of local platform water or porewater dissolved inorganic carbon that is not representative of the composition of seawater. The simplest explanation is that the BACE is younger than 538.04 \pm 0.14 Ma-the age of the ash bed at the top of the lower Nomtsas Formation that marks the end of carbonate sedimentation in the Nama Group. This is consistent with a younger age for the Ediacaran-Cambrian boundary than currently recognized, which, as suggested in Section 5.1, is also consistent with the absence of Treptichnus pedum in these units. Such an interpretation would imply that the 539.40 \pm 0.23 Ma U-Pb CA-ID-TIMS date from the horizon in the La Ciénega Formation of Sonora, Mexico just above the nadir of the BACE should be considered a maximum, rather than syn-, depositional age (Hodgin et al., 2021), that is >1 m.y. older than deposition of this unit. This would also imply that either the ash bed with the U-Pb CA-ID-TIMS date of 541.00 ± 0.13 Ma from the Ara Group of Oman (Bowring et al., 2007) is >3 m.y. older than the negative carbon isotope excursion just above it preserved in the A4 carbonate stringer, or that this is an older excursion, distinct from the BACE. This could be comparable to the recent interpretation of two stratigraphically discrete carbon isotope excursions in the Ediacaran successions of South China that were previously attributed to the single Shuram excursion (Yang et al., 2021).

If the BACE is in fact older than 538.04 \pm 0.14 Ma, as suggested by the dates from the La Ciénega Formation and/or the Ara Group, and contemporaneous with the deposition of the upper Nama Group, then a second possible explanation for the absence of a negative δ^{13} C excursion in the Huns or Spitskop members is that some or all of these carbonate rocks do not faithfully record secular changes in the δ^{13} C composition of coeval seawater. When un-

lithified carbonate sediment is transformed to limestone through neomorphism and diagenesis, this diagenetic system can range from fluid-buffered, whereby the compositions of diagenetic mineral phases resemble the diagenetic fluid, to sediment-buffered, whereby the compositions of the diagenetic mineral phases resemble the primary carbonate sediment (Higgins et al., 2018). A sediment-buffered diagenetic regime for the upper Nama Group is consistent with existing Ca isotope ($\delta^{44/40}$ Ca) and Sr concentration data for the Spitskop Member (Fig. 9B; Tostevin et al., 2019a), because sediment-buffered limestone preserves high Sr/Ca and low $\delta^{44/40}$ Ca of primary aragonite (Higgins et al., 2018). This mode of diagenetic influence, in which sediment pore fluids were more isolated from seawater, may have resulted from the extremely high sediment accumulation rates (~40 to 120 cm/kyr; Fig. 2)—for comparison, sediment accumulation rates for carbonates of the Ediacaran Ara Group of Oman are estimated at only 4 to 9 cm/kyr (Bowring et al., 2007). Sediment-buffered diagenesis would have promoted the preservation of primary sediment $\delta^{13}C$ signatures during neomorphism and lithification (Higgins et al., 2018). Therefore, if the δ^{13} C values of the Schwarzrand Subgroup are decoupled from primary marine values, these are unlikely to have resulted from diagenesis, but instead may have responded to local controls on the composition of dissolved inorganic carbon within restricted platform top waters or platform pore fluids, such as primary productivity and microbial metabolic effects (e.g., Geyman and Maloof, 2019; Nelson et al., 2021). Such an interpretation remains speculative, and, hence the bulk of evidence presently suggest that the BACE postdated deposition of carbonates of the Nama Group.

A decrease in $\delta^{44/40}$ Ca values from the lower carbonate units of the Nama Group (Omkyk Member of the Kuibis Subgroup) to the upper carbonate units of the Nama Group (Spitskop Member of the Schwarzrand Subgroup) was previously interpreted as representing a global change in the marine Ca isotope composition, potentially related to increased evaporate deposition or increased global weathering (Tostevin et al., 2019a). The Bayesian age-depth model for the Nama Group presented herein establishes a significant increase in sediment accumulation rate from the Kuibis Subgroup to the upper Schwarzrand Subgroup (Fig. 9A), which is consistent with typical subsidence of foreland basins that is classically thought to accelerate with time (e.g., DeCelles and Giles, 1996). Therefore, we suggest the decrease in $\delta^{44/40}$ Ca values and corresponding increase in Sr/Ca values resulted from a change in diagenetic regime from fluid-buffered to sediment-buffered marine diagenesis due to the increase in sedimentation rate, rather than any global change (Fig. 9A, B). A decrease in $\delta^{238/235}$ U values from carbonates of the Omkyk Member to the overlying Hoogland Member of the Zaris subbasin has been documented and interpreted as a global expansion of anoxia (Tostevin et al., 2019b). Similar to the change in $\delta^{44/40}$ Ca values, this decrease may instead have been caused by a change in diagenetic regime, driven by the acceleration of sediment accumulation within the Nama basin (Fig. 9A). This is because $\delta^{238/235}$ U values higher than seawater can be produced by pore water reduction of uranium in fluid-buffered diagenetic regimes with a plentiful uranium supply from seawater (Chen et al., 2018), while sediment-buffered carbonate minerals are more likely to preserve primary seawater $\delta^{238/235}$ U values (Chen et al., 2018; Tostevin et al., 2019b). As Tostevin et al. (2019b) recognize, the higher $\delta^{238/235}$ U values correspond to the highest $\delta^{44/40}$ Ca values within the lower Omkyk Member, consistent with this process (Fig. 9). Therefore, these higher $\delta^{238/235}$ U values were caused by seawater-buffered diagenesis, while the lower $\delta^{238/235}$ U values of the upper Omkyk and Hoogland members are the more faithful record of late Ediacaran marine oxygen levels, consistent with globally widespread seafloor anoxia (Tostevin et al., 2019a).

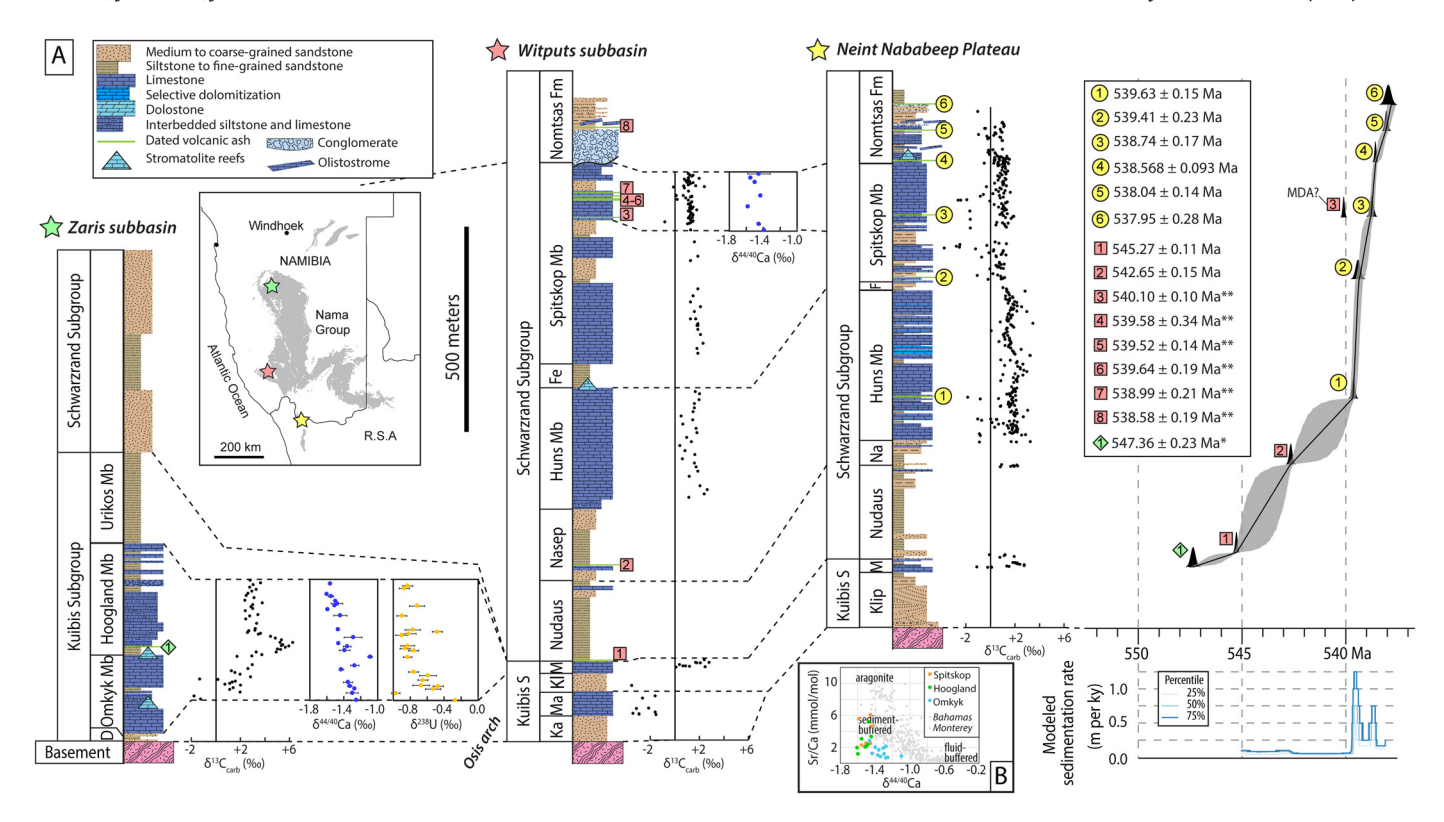


Fig. 9. A) Composite geochronology and chemostratigraphy of the Nama Group. Witputs and Zaris subbasin stratigraphy adapted from Saylor et al. (1995) and Grotzinger et al. (1995). Volcanic ash bed dates are weighted mean $^{206}\text{Pb}/^{238}\text{U}$ dates with internal 2σ uncertainties; *date from Bowring et al., 2007; **date from Linnemann et al., 2019; other geochronology data are from this paper. $\delta^{13}\text{C}$ data from Zaris subbasin from Wood et al. (2015); $\delta^{44/40}\text{Ca}$ data from Tostevin et al. (2019a); $\delta^{238}\text{U}$ data from Saylor et al. (1998), Ries et al. (2009), and Wood et al. (2015); $\delta^{13}\text{C}$ data from Neint Nababeep Plateau from this study. The Bchron Bayesian age-depth model is presented with its median (black line) and its 95% confidence interval (grey area). Modeled sedimentation rate does not account for delithification. B) Cross plot compares published Sr/Ca and $\delta^{44/40}\text{Ca}$ data from the Omkyk, Hoogland, and Spitskop members; data from Tostevin et al. (2019a) and Wood et al. (2015). Geochemical data from Miocene–Holocene carbonates from the Bahamas and authigenic dolomite from the Neogene Monterey Formation plotted for comparison (Blättler et al., 2015; Ahm et al., 2018; Higgins et al., 2018). Mb—Member; Fm—Formation; D—Dabis Formation; S—Subgroup; Ka—Kanies; Ma—Mara; Kl—Kliphoek; M—Mooifontein; Fe/F—Feldshuhhorn; Na—Nasep; MDA—Maximum Depositional Age.

6. Conclusions

The base of the Cambrian was one of the first recognized stratigraphic boundaries (originally thought to mark the end of an 'azoic' Precambrian epoch) and marks a particularly significant juncture in Earth history with the start of the Phanerozoic Eon. Nevertheless, the Ediacaran-Cambrian boundary remains a poorly understood geological transition, in terms of the tempo and relationships among environmental, evolutionary, and ecological change. This is largely because radioisotope geochronologic data for this interval remain scarce and correlating stratigraphic sections among, and even within, paleo-continents remains challenging.

New ash bed U-Pb CA-ID-TIMS geochronology from the Nama Group of the Neint Nababeep Plateau in the Republic of South Africa and the Witputs subbasin in Namibia allow for construction of, to date, the highest resolution age-stratigraphic model for global strata spanning c. 548 to 538 Ma. Limestones of the upper Schwarzrand Subgroup were deposited with relatively continuous and high rates of sedimentation from 539.78+0.63/-0.22 Ma to 538.04+0.14/-0.12 Ma, but do not preserve a negative δ^{13} C excursion that can be correlated to the BACE. This could be because of local controls on the dissolved inorganic carbon composition of surface waters and/or porewaters of this carbonate platform, or because the BACE is younger than currently recognized and occurred after 538.04+0.14/-0.12 Ma. Ediacaran-type fossils including erniettomorphs and cloudinomorphs occur in the Nomtsas Formation, after 538.56+0.08/-0.09 Ma, stratigraphically overlapping with relatively complex bilaterian trace fossils, such

as *Parapsammichnites*, *Archaeonassa*, *Psammichnites*, and treptichnids. However, we cannot discount at this time the possibility that the first occurrence of the index fossil *Treptichnus pedum* and thus the biostratigraphically defined Ediacaran-Cambrian boundary could postdate 537.9 Ma, condensing the duration of the early Cambrian. When placed in a global stratigraphic context, our results reveal the challenges of a purely biostratigraphic definition of the Ediacaran-Cambrian boundary and highlight the necessity of an integrated approach (chemostratigraphy, biostratigraphy, and radioisotopic geochronology) in reconstructing the tempo and patterns of evolution across this key interval of Earth history. The new age-stratigraphic model for the Nama Group provides a foundation for further temporal calibration of the terminal Ediacaran biostratigraphic and geochemical records.

CRediT authorship contribution statement

Lyle L. Nelson: Conceptualization, Funding acquisition, Investigation, Visualization, Writing – original draft. Jahandar Ramezani: Conceptualization, Data curation, Funding acquisition, Investigation, Resources, Writing – review & editing. John E. Almond: Investigation. Simon A.F. Darroch: Writing – review & editing. Wendy L. Taylor: Writing – review & editing. Dana C. Brenner: Data curation, Investigation, Writing – review & editing. Ryan P. Furey: Investigation. Madison Turner: Investigation, Writing – review & editing. Emily F. Smith: Conceptualization, Funding acquisition, Investigation, Supervision, Writing – review & editing.

Declaration of competing interest

The authors declare that they have no known competing financial interests or personal relationships that could have appeared to influence the work reported in this paper.

Acknowledgements

This project was funded by the National Science Foundation (NSF) grant EAR-1827715 to EFS and IR. LLN was supported by NSF Graduate Research Fellowship DGE-1746891 and the American Philosophical Society Lewis and Clark Fund for Exploration and Field Research. We thank the Johns Hopkins University (IHU) Department of Earth and Planetary Sciences for additional financial and logistical support. We thank the South African Heritage Resources Agency and the Geological Survey of Namibia for research and collection permits. We thank H. Mocke for permitting support. I. Bennett and R. Frazer are acknowledged for assistance in processing and analyzing samples in the MIT Isotope Lab, and A. Lindsay-Kaufman, L. Webb, and J. Thompson for assistance in processing and analyzing samples in the stable isotope laboratory at JHU. We are grateful to F. Macdonald and D. Schrag for supporting stable isotope analyses at Harvard University. R. Nel is acknowledged for field assistance. We are extremely grateful to R. Swart for logistical support, hospitality, and countless discussions about the geology of southern Africa. We are thankful to J. Grotzinger for discussions about the Nama Group and for leading a field trip to the Zaris subbasin in Namibia, and to K.-H. Hoffmann for discussions and logistical support. EFS and LLN thank P. Hoffman for generously loaning us his bakkie in 2016 to commence this study. We thank P. Hoffman and D. Erwin for comments on an earlier draft, two anonymous reviewers for critical feedback that improved this manuscript, and B. Wing for editorial assistance.

Appendix A. Supplementary material

Supplementary material related to this article can be found online at https://doi.org/10.1016/j.epsl.2022.117396.

References

- Ahm, A.C., Bjerrum, C.J., Blättler, C.L., Swart, P.K., Higgins, J.A., 2018. Quantifying early marine diagenesis in shallow-water carbonate sediments. Geochim. Cosmochim. Acta 236, 140–159.
- Almond, J.E., 2009. Contributions to the palaeontology and stratigraphy of the Alexander Bay sheet area (1: 250.000 geological sheet 2816). Unpublished report for the Council for Geoscience, Natura Viva cc, Cape Town. 117 p.
- Amthor, J.E., Grotzinger, J.P., Schröder, S., Bowring, S.A., Ramezani, J., Martin, M.W., Matter, A., 2003. Extinction of *Cloudina* and *Namacalathus* at the Precambrian-Cambrian boundary in Oman. Geology 31 (5), 431–434.
- Blanco, G., Germs, G.J.B., Rajesh, H.M., Chemale Jr, F., Dussin, I.A., Justino, D., 2011. Provenance and paleogeography of the Nama Group (Ediacaran to early Palaeozoic, Namibia): petrography, geochemistry and U–Pb detrital zircon geochronology. Precambrian Res. 187 (1–2), 15–32.
- Blättler, C.L., Miller, N.R., Higgins, J.A., 2015. Mg and Ca isotope signatures of authigenic dolomite in siliceous deep-sea sediments. Earth Planet. Sci. Lett. 419, 32–42.
- Bowring, S.A., Grotzinger, J.P., Condon, D.J., Ramezani, J., Newall, M.J., Allen, P.A., 2007. Geochronologic constraints on the chronostratigraphic framework of the Neoproterozoic Huqf Supergroup, Sultanate of Oman. Am. J. Sci. 307 (10), 1097–1145.
- Brasier, M., Cowie, J., Taylor, M., 1994. Decision on the Precambrian-Cambrian boundary stratotype, Episodes. J. Int. Geosci. 17 (1), 3–8.
- Brasier, M.D., Shields, G., Kuleshov, V.N., Zhegallo, E.A., 1996. Integrated chemoand biostratigraphic calibration of early animal evolution: Neoproterozoic-early Cambrian of southwest Mongolia. Geol. Mag. 133, 445–485. https://doi.org/10. 1017/S0016756800007603.
- Buatois, L.A., Almond, J., Mángano, M.G., Jensen, S., Germs, G.J., 2018. Sediment disturbance by Ediacaran bulldozers and the roots of the Cambrian explosion. Sci. Rep. 8 (1), 1–9.

- Chen, X., Romaniello, S.J., Herrmann, A.D., Hardisty, D., Gill, B.C., Anbar, A.D., 2018. Diagenetic effects on uranium isotope fractionation in carbonate sediments from the Bahamas. Geochim. Cosmochim. Acta 237, 294–311. https://doi.org/10.1016/j.gca.2018.06.026.
- Cohen, P.A., Bradley, A., Knoll, A.H., Grotzinger, J.P., Jensen, S., Abelson, J., Hand, K., Love, G., Metz, J., McLoughlin, N., Meister, P., 2009. Tubular compression fossils from the Ediacaran Nama group, Namibia. J. Paleontol. 83 (1), 110–122.
- Condon, D., Zhu, M., Bowring, S., Wang, W., Yang, A., Jin, Y., 2005. U-Pb ages from the neoproterozoic Doushantuo Formation. China. Science 308 (5718), 95-98.
- Corsetti, F.A., Hagadorn, J.W., 2000. Precambrian-Cambrian transition: Death Valley, United States. Geology 28, 299–302.
- Crimes, T.P., Germs, G.J., 1982. Trace fossils from the Nama Group (Precambrian-Cambrian) of Southwest Africa (Namibia). J. Paleontol. 56 (4), 890-907.
- Darroch, S.A., Boag, T.H., Racicot, R.A., Tweedt, S., Mason, S.J., Erwin, D.H., Laflamme, M., 2016. A mixed Ediacaran-metazoan assemblage from the Zaris Sub-basin, Namibia. Palaeogeogr. Palaeoclimatol. Palaeoecol. 459, 198–208.
- Darroch, S.A., Smith, E.F., Laflamme, M., Erwin, D.H., 2018. Ediacaran extinction and Cambrian explosion. Trends Ecol. Evol. 33 (9), 653–663.
- Darroch, S.A., Cribb, A.T., Buatois, L.A., Germs, G.J., Kenchington, C.G., Smith, E.F., Mocke, H., O'Neil, G.R., Schiffbauer, J.D., Maloney, K.M., Racicot, R.A., Turk, K.A., Gibson, B.M., Almond, J., Koester, B., Boag, T.H., Tweedt, S.M., Laflamme, M., 2021. The trace fossil record of the Nama Group, Namibia: exploring the terminal Ediacaran roots of the Cambrian explosion. Earth-Sci. Rev. 212, 103435.
- DeCelles, P.G., Giles, K.A., 1996. Foreland basin systems. Basin Res. 8 (2), 105-123.
- Germs, G.J.B., Gresse, P.G., 1991. The foreland basin of the Damara and Gariep orogens in Namaqualand and southern Namibia: stratigraphic correlations and basin dynamics. S. Afr. J. Geol. 94 (2), 159–169.
- Germs, G.J.B., 1972. Trace fossils from the Nama Group, South-West Africa. J. Paleontol. 46 (6), 864–870.
- Germs, G.J.B., 1983. Implications of a sedimentary facies and depositional environmental analysis of the Nama Group in Southwest Africa/Namibia. In: Miller, R. McG. (Ed.), Evolution of the Damara Orogen. In: Geological Society of South Africa, Special Publication, vol. 11, pp. 89–114.
- Germs, G.J.B., Miller, R.McG., Frimmel, H.E., Gaucher, C., 2009. Syn- to late-orogenic sedimentary basins of Southwestern Africa. In: Gaucher, C., Sial, A.N., Halverson, G.P., Frimmel, H.E. (Eds.), Neoproterozoic-Cambrian Tectonics, Global Change and Evolution: A Focus on Southwestern Gondwana. Elsevier.
- Geyer, G., 2005. The fish river subgroup in Namibia: stratigraphy, depositional environments and the Proterozoic-Cambrian boundary problem revisited. Geol. Mag. 142 (5), 465-498.
- Geyer, G., Uchman, A., 1995. Ichnofossil assemblages from the Nama Group (Neoproterozoic-Lower Cambrian) in Namibia and the Proterozoic-Cambrian boundary problem revisited. In: Geyer, G., Landing, E. (Eds.), Morocco '95 the Lower-Middle Cambrian Standard of Western Gondwana, Beringeria Special Issue 2, pp. 175–202.
- Geyman, E.C., Maloof, A.C., 2019. A diurnal carbon engine explains ¹³C-enriched carbonates without increasing the global production of oxygen. Proc. Natl. Acad. Sci. 116 (49), 24433–24439.
- Gresse, P.G., Germs, G.J.B., 1993. The Nama foreland basin: sedimentation, major unconformity bounded sequences and multisided active margin advance. Precambrian Res. 63 (3–4), 247–272.
- Gresse, P.G., von Veh, M.W., Frimmel, H.E., 2006. Namibian (Neoproterozoic) to Early Cambrian successions. In: Johnson, M.R., Anhaeusser, C.R., Thomas, R.J. (Eds.), The Geology of South Africa. Geological Society of South Africa, Johannesburg/Council for Geoscience, Pretoria, pp. 395–420.
- Grotzinger, J.P., 2000. Facies and paleoenvironmental setting of thrombolitestromatolite reefs, terminal Proterozoic Nama Group (ca. 550–543 Ma), central and southern Namibia. Commun. Geol. Surv. Namib. 12, 221–233.
- Grotzinger, J.P., Bowring, S.A., Saylor, B.Z., Kaufman, A.J., 1995. Biostratigraphic and geochronologic constraints on early animal evolution. Science 270 (5236), 598–604
- Grotzinger, J., Adams, E.W., Schröder, S., 2005. Microbial-metazoan reefs of the terminal Proterozoic Nama Group (c. 550-543 Ma), Namibia. Geol. Mag. 142 (5), 499-517.
- Higgins, J.A., Blättler, C.L., Lundstrom, E.A., Santiago-Ramos, D.P., Akhtar, A.A., Ahm, A.C., Bialik, O., Holmden, C., Bradbury, H., Murray, S.T., Swart, P.K., 2018. Mineralogy, early marine diagenesis, and the chemistry of shallow-water carbonate sediments. Geochim. Cosmochim. Acta 220, 512–534.
- Hodgin, E.B., Nelson, L.L., Wall, C.J., Barrón-Díaz, A.J., Webb, L.C., Schmitz, M.D., Fike, D.A., Hagadorn, J.W., Smith, E.F., 2021. A link between rift-related volcanism and end-Ediacaran extinction? Integrated chemostratigraphy, biostratigraphy, and U-Pb geochronology from Sonora, Mexico. Geology 49 (2), 115–119.
- Ivantsov, A.Y., 2013. New data on Late Vendian problematic fossils from the genus *Harlaniella*. Stratigr. Geol. Correl. 21, 592–600.
- Jaffey, A.H., Flynn, K.F., Glendenin, L.E., Bentley, W.C., Essling, A.M., 1971. Precision measurement of half-lives and specific activities of ²³⁵U and ²³⁸U. Phys. Rev. C 4 (5), 1889–1906.
- Jensen, S., Runnegar, B.N., 2005. A complex trace fossil from the Spitskop Member (terminal Ediacaran-? Lower Cambrian) of southern Namibia. Geol. Mag. 142 (5), 561–569.

- Jensen, S., Saylor, B.Z., Gehling, J.G., Germs, G.J., 2000. Complex trace fossils from the terminal Proterozoic of Namibia. Geology 28 (2), 143–146.
- Jensen, S., Högström, A.E.S., Almond, J., Taylor, W.L., Meinhold, G., Høyberget, M., Ebbestad, J.O.R., Agić, H., Palacios, T., 2018. Scratch circles from the Ediacaran and Cambrian of Arctic Norway and southern Africa, with a review of scratch circle occurrences. Bull. Geosci. 93 (3), 287–304.
- Kim, Y., Lee, C., Lee, E.Y., 2018. Numerical analysis of sedimentary compaction: implications for porosity and layer thickness variation. J. Geol. Soc. Korea 54, 631–640. https://doi.org/10.14770/jgsk.2018.54.6.631.
- Laflamme, M., Darroch, S.A., Tweedt, S.M., Peterson, K.J., Erwin, D.H., 2013. The end of the Ediacara biota: extinction, biotic replacement, or Cheshire Cat? Gondwana Res. 23 (2), 558–573.
- Linnemann, U., Ovtcharova, M., Schaltegger, U., Gärtner, A., Hautmann, M., Geyer, G., Vickers-Rich, P., Rich, T., Plessen, B., Hofmann, M., Zieger, J., 2019. New high-resolution age data from the Ediacaran-Cambrian boundary indicate rapid, ecologically driven onset of the Cambrian explosion. Terra Nova 31 (1), 49–58.
- MacNaughton, R.B., Fallas, K.M., Finley, T.D., 2021. Psammichnites gigas from the lower Cambrian of the Mackenzie Mountains, northwest Canada, and their biostratigraphic implications. Ichnos 28 (3), 164–175.
- Mehra, A., Watters, W.A., Grotzinger, J.P., Maloof, A.C., 2020. Three-dimensional reconstructions of the putative metazoan Namapoikia show that it was a microbial construction. Proc. Natl. Acad. Sci. 117 (33), 19760–19766.
- Narbonne, G.M., Kaufman, A.J., Knoll, A.H., 1994. Integrated chemostratigraphy and biostratigraphy of the Windermere Supergroup, northwestern Canada: implications for Neoproterozoic correlations and the early evolution of animals. Geol. Soc. Am. Bull. 106. 1281–1292.
- Narbonne, G.M., Saylor, B.Z., Grotzinger, J.P., 1997. The youngest Ediacaran fossils from Southern Africa. J. Paleontol. 71, 953–967.
- Nelson, L.L., Ahm, A.S.C., Macdonald, F.A., Higgins, J.A., Smith, E.F., 2021. Fingerprinting local controls on the Neoproterozoic carbon cycle with the isotopic record of Cryogenian carbonates in the Panamint Range, California. Earth Planet. Sci. Lett. 566, 116956.
- Newstead, B.L., 2010. The Congo-Kalahari cratonic relationship: from Rodinia to Gondwana. M.S. Thesis. University of Florida, Gainesville. 234 p.
- Peng, S.C., Babcock, L.E., Ahlberg, P., 2020. Chapter 19 The Cambrian period. In: Gradstein, M., Ogg, J.G., Schmitz, M.D., Ogg, G.M. (Eds.), Geologic Time Scale 2020. Elsevier, pp. 565–629.
- Pflug, H.D., 1970. Zur Fauna der Nama-Schichten in Südwest Afrika I. Pteridinia, Bau und Systematische Zugehörigkeit. Palaeontogr. Abt. A 134, 226–262.
- Pflug, H.D., 1972. Zur Fauna der Nama-Schichten in Südwest-Afrika. III. Erniettomorpha, Bau und Systematik. Palaeontogr. Abt. A 139, 134–170.
- Ries, J.B., Fike, D.A., Pratt, L.M., Lyons, T.W., Grotzinger, J.P., 2009. Superheavy pyrite $(\delta^{34} S_{pyr} > \delta^{34} S_{CAS})$ in the terminal Proterozoic Nama Group, southern Namibia: a consequence of low seawater sulfate at the dawn of animal life. Geology 37 (8), 743–746.
- Rooney, A.D., Cantine, M.D., Bergmann, K.D., Gómez-Pérez, I., Al Baloushi, B., Boag, T.H., Busch, J.F., Sperling, E.A., Strauss, J.V., 2020. Calibrating the coevolution of Ediacaran life and environment. Proc. Natl. Acad. Sci. 117 (29), 16824–16830.
- Saylor, B.Z., 2003. Sequence stratigraphy and carbonate-siliciclastic mixing in a terminal Proterozoic foreland basin, Urusis Formation, Nama Group, Namibia. J. Sediment. Res. 73 (2), 264–279.

- Saylor, B.Z., Grotzinger, J.P., 1996. Reconstruction of important Proterozoic-Cambrian boundary exposures through the recognition of thrust deformation in the Nama Group of southern Namibia. Commun. Geol. Surv. Namib. 11, 1–12.
- Saylor, B.Z., Grotzinger, J.P., Germs, G.J.B., 1995. Sequence stratigraphy and sedimentology of the Neoproterozoic Kuibis and Schwarzrand subgroups (Nama Group), southwestern Namibia. Precambrian Res. 73 (1–4), 153–171.
- Saylor, B.Z., Kaufman, A.J., Grotzinger, J.P., Urban, F., 1998. A composite reference section for terminal Proterozoic strata of southern Namibia. J. Sediment. Res. 68 (6), 1223–1235.
- Saylor, B.Z., Poling, J.M., Huff, W.D., 2005. Stratigraphic and chemical correlation of volcanic ash beds in the terminal Proterozoic Nama Group, Namibia. Geol. Mag. 142 (5), 519–538.
- Seilacher, A., 2007. Trace Fossil Analysis. Springer, Heidelberg.
- Smith, E.F., Nelson, L.L., Strange, M.A., Eyster, A.E., Rowland, S.M., Schrag, D.P., Macdonald, F.A., 2016. The end of the Ediacaran: two new exceptionally preserved body fossil assemblages from Mount Dunfee, Nevada, USA. Geology 44 (11), 911–914.
- Smith, E.F., Nelson, L.L., Tweedt, S.M., Zeng, H., Workman, J.B., 2017. A cosmopolitan late Ediacaran biotic assemblage: new fossils from Nevada and Namibia support a global biostratigraphic link. Proc. R. Soc. Lond. B, Biol. Sci. 284 (1858), 20170934.
- Tostevin, R., Bradbury, H.J., Shields, G.A., Wood, R.A., Bowyer, F., Penny, A.M., Turchyn, A.V., 2019a. Calcium isotopes as a record of the marine calcium cycle versus carbonate diagenesis during the late Ediacaran. Chem. Geol. 529, 119319.
- Tostevin, R., Clarkson, M.O., Gangl, S., Shields, G.A., Wood, R.A., Bowyer, F., Penny, A.M., Stirling, C.H., 2019b. Uranium isotope evidence for an expansion of anoxia in terminal Ediacaran oceans. Earth Planet. Sci. Lett. 506, 104–112.
- Wilson, J.P., Grotzinger, J.P., Fischer, W.W., Hand, K.P., Jensen, S., Knoll, A.H., Abelson, J., Metz, J.M., McLoughlin, N., Cohen, P.A., Tice, M.M., 2012. Deep-water incised valley deposits at the Ediacaran-Cambrian boundary in southern Namibia contain abundant *Treptichnus pedum*. Palaios 27 (4), 252–273.
- Wood, R.A., Grotzinger, J.P., Dickson, J.A.D., 2002. Proterozoic modular biomineralized metazoan from the Nama Group, Namibia. Science 296 (5577), 2383–2386.
- Wood, R.A., Poulton, S.W., Prave, A.R., Hoffmann, K.H., Clarkson, M.O., Guilbaud, R., Lyne, J.W., Tostevin, R., Bowyer, F., Penny, A.M., Curtis, A., 2015. Dynamic redox conditions control late Ediacaran metazoan ecosystems in the Nama Group, Namibia. Precambrian Res. 261, 252–271.
- Yang, B., Steiner, M., Zhu, M., Li, G., Liu, J., Liu, P., 2016. Transitional Ediacaran-Cambrian small skeletal fossil assemblages from South China and Kazakhstan: implications for chronostratigraphy and metazoan evolution. Precambrian Res. 285, 202–215.
- Yang, C., Rooney, A.D., Condon, D.J., Li, X.H., Grazhdankin, D.V., Bowyer, F.T., Hu, C., Macdonald, F.A., Zhu, M., 2021. The tempo of Ediacaran evolution. Sci. Adv. 7 (45), eabi9643.
- Zhang, J., Li, G., Zhou, C., Zhu, M., Yu, Z., 1997. Carbon isotope profiles and their correlation across the Neoproterozoic-Cambrian boundary interval on the Yangtze Platform, China. Bull. Natl. Museum Nat. Sci. 10, 107–116.
- Zhu, M., Zhuravlev, A.Y., Wood, R.A., Zhao, F., Sukhov, S.S., 2017. A deep root for the Cambrian explosion: implications of new bio- and chemostratigraphy from the Siberian Platform. Geology 45 (5), 459–462. https://doi.org/10.1130/g38865.1.